Original Article | Cardiovascular Imaging

eISSN 2005-8330
https://doi.org/10.3348/kjr.2023.0065
Korean J Radiol 2023;24(5):395-405

Korean Journal of Radiology
KJR

T1 Map-Based Radiomics for Prediction of Left Ventricular Reverse Remodeling in Patients With Nonischemic Dilated Cardiomyopathy

Suyon Chang[1,2], Kyunghwa Han[1], Yonghan Kwon[1], Lina Kim[1], Seunghyun Hwang[1], Hwiyoung Kim[1], Byoung Wook Choi[1]

[1]Department of Radiology, Research Institute of Radiological Science, Center for Clinical Imaging Data Science, Yonsei University College of Medicine, Seoul, Korea
[2]Department of Radiology, Seoul St. Mary's Hospital, College of Medicine, The Catholic University of Korea, Seoul, Korea

Objective: This study aimed to develop and validate models using radiomics features on a native T1 map from cardiac magnetic resonance (CMR) to predict left ventricular reverse remodeling (LVRR) in patients with nonischemic dilated cardiomyopathy (NIDCM).

Materials and Methods: Data from 274 patients with NIDCM who underwent CMR imaging with T1 mapping at Severance Hospital between April 2012 and December 2018 were retrospectively reviewed. Radiomic features were extracted from the native T1 maps. LVRR was determined using echocardiography performed ≥ 180 days after the CMR. The radiomics score was generated using the least absolute shrinkage and selection operator logistic regression models. Clinical, clinical + late gadolinium enhancement (LGE), clinical + radiomics, and clinical + LGE + radiomics models were built using a logistic regression method to predict LVRR. For internal validation of the result, bootstrap validation with 1000 resampling iterations was performed, and the optimism-corrected area under the receiver operating characteristic curve (AUC) with 95% confidence interval (CI) was computed. Model performance was compared using AUC with the DeLong test and bootstrap.

Results: Among 274 patients, 123 (44.9%) were classified as LVRR-positive and 151 (55.1%) as LVRR-negative. The optimism-corrected AUC of the radiomics model in internal validation with bootstrapping was 0.753 (95% CI, 0.698–0.813). The clinical + radiomics model revealed a higher optimism-corrected AUC than that of the clinical + LGE model (0.794 vs. 0.716; difference, 0.078 [99% CI, 0.003–0.151]). The clinical + LGE + radiomics model significantly improved the prediction of LVRR compared with the clinical + LGE model (optimism-corrected AUC of 0.811 vs. 0.716; difference, 0.095 [99% CI, 0.022–0.139]).

Conclusion: The radiomic characteristics extracted from a non-enhanced T1 map may improve the prediction of LVRR and offer added value over traditional LGE in patients with NIDCM. Additional external validation research is required.

Keywords: Cardiomyopathy, Dilated; Magnetic resonance imaging; Prognosis; Radiomics

INTRODUCTION

Nonischemic dilated cardiomyopathy (NIDCM) is a common myocardial disease defined by the presence of left ventricular dilatation and left ventricular systolic dysfunction in the absence of abnormal loading conditions such as hypertension, valve disease, or coronary artery disease sufficient to cause global systolic impairment [1]. The prognosis of the disease has remarkably improved in recent decades with optimal medical therapy, and some patients undergo left ventricular reverse remodeling (LVRR), which is characterized by a decrease in dimensions and an improvement in pump function [2]. Since LVRR is associated with a favorable long-term prognosis [2,3], its prediction

Received: October 12, 2022 **Revised:** February 3, 2023 **Accepted:** February 26, 2023
Corresponding author: Byoung Wook Choi, MD, PhD, Department of Radiology, Research Institute of Radiological Science, Center for Clinical Imaging Data Science, Yonsei University College of Medicine, 50-1 Yonsei-ro, Seodaemun-gu, Seoul 03722, Korea.
• E-mail: bchoi@yuhs.ac

can help in risk stratification and treatment planning. This has led to extensive research regarding prediction of LVRR with clinical and cardiac magnetic resonance (CMR) data, including age, systolic blood pressure, B-type natriuretic peptide (BNP) level, New York Heart Association (NYHA) class, left ventricular ejection fraction (LVEF), presence or extent of late gadolinium enhancement (LGE), and mapping values [2,4-7].

Traditionally, LGE has been recognized as a strong prognostic factor in dilated cardiomyopathy (DCM) patients [8]. However, the assessment of LGE can be reader-dependent and is limited in the evaluation of diffuse interstitial fibrosis, which is common in DCM [9]. Furthermore, the use of gadolinium-based contrast media is limited in patients with severe renal dysfunctions. In contrast, the native T1 map provides quantitative information for detecting diffuse myocardial disease without the use of contrast media. Prior studies reported that native T1 had predictive value for prognosis in non-ischemic cardiomyopathy [10,11]. However, the primary endpoint of these studies was all-cause mortality or ventricular arrhythmias. According to a recent study, the baseline native T1 value was not a significant predictor of LVRR in DCM patients [7]. Considering these results, a novel method to maximize the utilization of native T1 is required to predict functional recovery without contrast media.

Radiomics enables the comprehensive evaluation of imaging by extracting and mining a large number of quantitative image features, including shape, intensity distribution, spatial relationships between various intensity levels, and texture heterogeneity patterns [12]. The main goal of radiomics analysis is to provide accurate risk stratification by incorporating imaging traits into predictive models for outcomes and evaluating their added value to commonly used predictors [13]. Some prior studies have reported that combined myocardial tissue heterogeneity and interstitial fibrosis assessment by native T1 mapping showed a good prognostic ability comparable to that of enhanced images [14,15], suggesting the potential of radiomics analysis of the native T1 map. This study aimed to develop and validate models using radiomics features on native T1 maps from CMR imaging to predict LVRR in patients with NIDCM.

MATERIALS AND METHODS

This retrospective study was approved by the Institutional

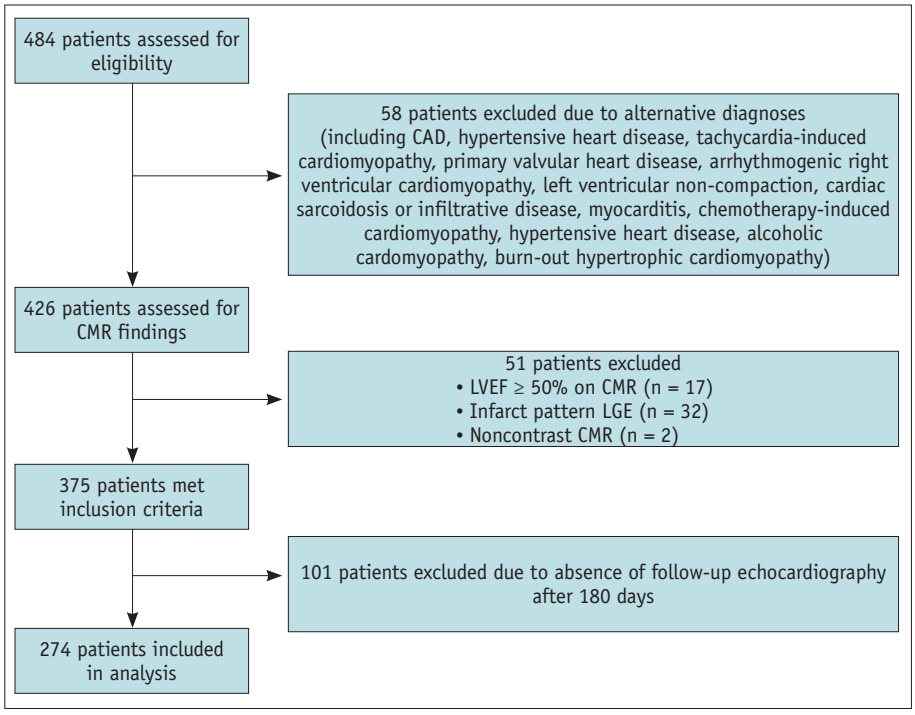

Fig. 1. Study participants. From 484 patients who underwent cardiac magnetic resonance (CMR) for suspected dilated cardiomyopathy (DCM), those with an alternative diagnosis, left ventricular ejection fraction (LVEF) ≥ 50%, an infarct pattern of late gadolinium enhancement (LGE), or who underwent noncontrast CMR were excluded. Additionally, patients who did not undergo follow-up echocardiography after 180 days were also excluded. Finally, 274 patients were included in the study. CAD = coronary artery disease

https://doi.org/10.3348/kjr.2023.0065

Korean Journal of Radiology
KJR

Review Board of Severance Hospital (IRB No. 1-2018-0077). The requirement for informed consent was waived.

Study Participants

The patient enrollment process is shown in Figure 1. Data from consecutive patients (n = 484) who underwent CMR for suspected DCM between April 2012 and December 2018 at Severance Hospital were reviewed. Patients were excluded if they had ischemic heart disease, defined as significant documented coronary artery disease or a previous history of myocardial infarction, hypertensive heart disease, tachycardia-induced cardiomyopathy, primary valvular heart disease, arrhythmogenic right ventricular cardiomyopathy, left ventricular non-compaction, cardiac sarcoidosis or infiltrative disease, myocarditis, chemotherapy-induced cardiomyopathy, hypertensive heart disease, alcoholic cardiomyopathy, or burn-out hypertrophic cardiomyopathy. Additional exclusion criteria were LVEF ≥ 50% on CMR, infarct pattern of LGE, or non-contrast CMR. Further, patients who did not undergo follow-up echocardiography after 180 days were also excluded. Finally, 274 patients were included in this study. Electronic medical records were reviewed for follow-up after CMR imaging for a minimum of 180 days. Echocardiography performed closest to 12 months after CMR was used for analysis. The development of LVRR was defined as an increase in LVEF by ≥ 10% combined with a decrease in left ventricular end-diastolic diameter index (LVEDDi) by ≥ 10% at follow-up ≥ 180 days after CMR.

Clinical and Echocardiographic Data

Clinical data collected for each patient included age, sex, body mass index (BMI) (kg/m^2), heart rate (beats/min), systolic blood pressure, diastolic blood pressure, creatinine level, estimated glomerular filtration rate (eGFR), sodium level, N-terminal prohormone B-type natriuretic peptide (NT-proBNP) level, diabetes, atrial fibrillation, smoking status, and family history of cardiomyopathy or sudden cardiac death. Echocardiographic data included LVEF and LVEDDi.

CMR Image Acquisition

All cardiac magnetic resonance (CMR) images were obtained using a 3-T MR imaging unit (Magnetom Trio; Siemens Healthineers) with an eight-channel cardiac coil. T1 mapping images were acquired before contrast injection in three short-axis planes (basal, mid, and apical LV) using a modified look-locker inversion-recovery (MOLLI) sequence at the end-expiratory phase. A nonselective inversion pulse (TrueFISP single-shot readout sequence in the mid-diastolic phase) was employed. A fully automated, non-rigid motion correction was applied to register individual T1 images before inline T1 fitting was performed using a mono-exponential three-parameter fit. Delayed enhancement imaging was performed 10 min after the injection of gadobutrol (0.2 mmol/kg, Gadovist; Bayer Healthcare) at a rate of 2 mL/s with a segmented inversion-recovery prepared turbo fast low-angle shot sequence in the short-axis plane. Data acquisition was synchronized with electrocardiogram in the mid-diastolic phase to minimize motion artifacts. A nonselective 180° pulse was applied after a trigger delay dependent on the heart rate. The inversion time was determined using the inversion scout sequence to nullify the signal intensity of the normal myocardium after contrast material injection. The imaging parameters are summarized in Supplementary Material.

CMR Image Analysis

The flow of this investigation is illustrated in Figure 2. The presence, extent, location (septal wall only, non-septal wall only, both septal and non-septal walls, or right ventricular insertion point [RVIP] only), and pattern (subendocardial, mid-wall, subepicardial, transmural, focal, or multiple) of LGE were assessed by a cardiac radiologist with 10-year experience who was blinded to the participant data. The endocardial and epicardial borders of the LV were manually delineated on short-axis LGE images. Myocardial LGE was defined as areas with signal intensity greater than five standard deviations (SDs) above the mean signal intensity of normal myocardium and expressed as a percentage of LV mass [16]. The recovery rate of T1 relaxation was measured in a mid-ventricular short-axis slice of the interventricular septum by a blinded and experienced observer. All image analyses were performed using CVI42 MR analysis software (Circle Cardiovascular Imaging Inc.).

Radiomics Feature Analysis

A native T1 map (mid-ventricular short axis) was exported as a single Digital Imaging and Communications in Medicine image for further analysis, and regions of interest encompassing the entire left ventricular myocardium were drawn by an experienced observer who was blinded to the participant data. Trabeculated and epicardial borders were carefully excluded to avoid partial volume effects. Visually appreciable artifacts were excluded from the region of interest.

 https://doi.org/10.3348/kjr.2023.0065

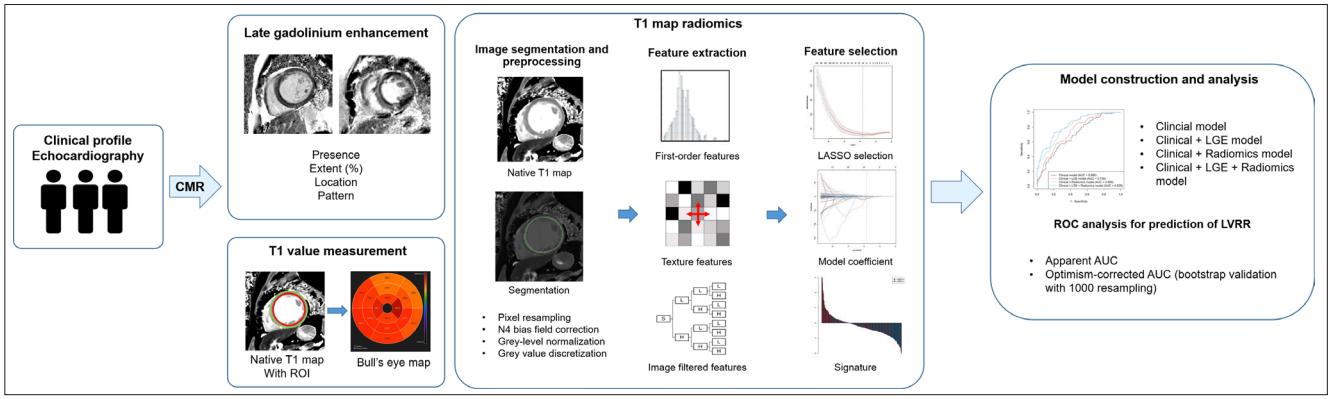

Fig. 2. The study workflow. Prediction models were constructed using cardiac magnetic resonance (CMR) with radiomics features on native T1 map for left ventricular reverse remodeling (LVRR) in patients with nonischemic dilated cardiomyopathy. The model performance was compared using the area under the receiver operating characteristic curve (AUC) with the DeLong test. For internal validation of the results, bootstrap validation with 1000 resampling iterations was performed, and optimism-corrected AUC with 95% confidence intervals were computed. LGE = late gadolinium enhancement, ROC = receiver operating characteristic, ROI = region of interest, LASSO = least absolute shrinkage and selection operator

Image preprocessing and feature extraction were performed by the SimpleITK Python package [17] according to the image biomarker standardization initiative (IBSI) recommendations [18]. Pixel resampling was performed at 1 x 1 mm^2 for all images because variations in pixel size can substantially affect the performance of texture features and reduce reproducibility [19]. Next, N4 bias field correction was performed to remove low-frequency intensity nonuniformity from images. Gray-level normalization was performed by rescaling the histogram data to fit within $\mu \pm 3\sigma$ (μ = gray-level mean, σ = gray-level SD) to minimize the effects of brightness and contrast variations and to correct for small technical intra- and inter-scanner fluctuations [20]. Gray value discretization was performed with a bin width of 5.

The radiomics features in this study were first-order, texture, and image-filtered features. First-order and textural features were obtained from the original and filtered images. Texture features included the gray-level co-occurrence matrix (GLCM), gray-level run length matrix (GLRLM), gray-level size-zone matrix (GLSZM), and neighboring gray-tone-difference matrix (NGTDM). The image filtered types applied were wavelet transformation, square, square root, logarithmic, exponential, gradient, and local binary pattern-2D (LBP-2D). A total of 869 features were extracted and analyzed. A list of the specific features in each category is included in Supplementary Table 1.

For feature selection, the least absolute shrinkage and selection operator (LASSO) was performed with 10-fold cross-validation to overcome the overfitting problem, and features showing nonzero coefficients using LASSO logistic regression were selected. Features were selected if the mean of the calculated area under the receiver operating characteristic (ROC) curve (AUC) was equivalent to the maximum value during cross-validation. A radiomics score (rad-score) was calculated for each case via a linear combination of selected features weighted by their respective coefficients calculated by the LASSO logistic regression model. Feature selection was performed using R (version 4.1.2.; R Foundation for Statistical Computing) and the "glmnet" package.

Statistical Analysis and Model Construction

Statistical analysis was performed using the SPSS software (version 24.0; IBM Corp.) and R (version 4.1.2., R Foundation for Statistical Computing). Categorical variables are presented as numbers and percentages. Continuous variables are presented as mean ± SD. Demographics, echocardiographic, and CMR findings were compared between the LVRR-positive and LVRR-negative groups by chi-square test or Fisher's exact test for categorical variables and independent *t*-test for continuous variables. Univariable and multivariable logistic regression analyses were performed to predict the LVRR.

We constructed prediction models for the LVRR. For the clinical model, bootstrapping with 300 resampling iterations was performed to select variables for the multivariable model. Variables selected in > 50% of the bootstrap procedures were entered into the subsequent multivariable model. For the clinical + LGE model, the variables in the clinical model and the conventional CMR variables with $P < 0.05$ in the univariable analyses were added to the multivariable model. In addition to the model using clinical and radiomics variables, a combined model was developed to

https://doi.org/10.3348/kjr.2023.0065

Korean Journal of Radiology
KJR

evaluate the prediction performance of all four models and the incremental value of the radiomics features.

ROC curves were generated to evaluate the performance of each model. For internal validation of the results, we performed bootstrap validation with 1000 resampling iterations to achieve optimism-corrected AUC with 95% confidence interval (CI) [21,22]. The optimism-corrected AUC difference was calculated using 1000 bootstrap samples. Model performance was compared using AUC with the DeLong test and bootstrap. The Bonferroni correction was applied for multiple comparisons. Statistical significance was set at $P < 0.05$.

RESULTS

Clinical Characteristics and Conventional CMR Findings

Table 1 shows the clinical characteristics and CMR data of the patients with and without LVRR. Among the 274 patients, 123 (44.9%) were classified as LVRR-positive and 151 (55.1%) were classified as LVRR-negative. Among the clinical and echocardiographic findings, Ln NT-proBNP, baseline LVEF, and baseline LVEDDi were significantly different between the LVRR positive and LVRR-negative group ($P = 0.006$, < 0.001, and < 0.001, respectively). Clinical variables such as age, sex, BMI, systolic and diastolic blood pressure, creatinine level, eGFR, sodium level, diabetes, smoking status, family history, atrial fibrillation, and the median follow-up interval were not significantly different between the two groups. Among the CMR data, the presence of LGE was more frequent in the LVRR-negative group, but the difference was not statistically significant (41.5% vs. 49%, $P = 0.212$). The extent of LGE differed significantly between the LVRR positive and LVRR-negative group (3.3% ± 7.0% vs. 7.6% ± 12.7%, $P = 0.014$). The LVRR-negative group had more frequent LGE in both walls, whereas the LVRR-positive group had more frequent LGE in the RVIP only group. The proportion of LGE patterns differed between the two groups ($P = 0.003$). The LVRR-negative group had more frequent mid-wall or multiple patterns of LGE, whereas the LVRR-positive group had more frequent focal LGE. Septal mid-wall LGE was more frequent in the LVRR-negative group (36.4% vs. 22%, $P = 0.014$) (Fig. 3). Native T1 value (1352.2 ± 73.9 ms vs. 1344.8 ± 84.6 ms, $P = 0.441$) was not significantly different between the LVRR positive and LVRR negative group (Fig. 4).

Table 1. Clinical Characteristics and Cardiac Magnetic Resonance Data in the LVRR Positive and Negative Groups

Variables	LVRR (-) (n = 151, 55.1%)	LVRR (+) (n = 123, 44.9%)	*P*
Clinical data			
Age, yr	56.1 ± 15.6	53.3 ± 17.3	0.221
Female	60 (39.7)	44 (35.8)	0.501
Body mass index, kg/m^2	24.7 ± 5.0	24.9 ± 4.7	0.498
Systolic blood pressure, mmHg	113.3 ± 16.0	117.1 ± 17.4	0.085
Diastolic blood pressure, mmHg	71.7 ± 11.6	73.8 ± 13.7	0.329
Creatinine, mg/dL	1.0 ± 0.8	1.2 ± 1.3	0.319
eGFR, mL/min/1.73 m^2	86.6 ± 26.9	84.9 ± 31.4	0.890
Sodium, mmol/L	140.4 ± 15.8	141.4 ± 16.3	0.847
Ln NT-proBNP, pg/mL	7.0 ± 1.5	7.5 ± 1.5	0.006†
Diabetes	37 (24.5)	24 (19.5)	0.323
Smoking	67 (44.4)	66 (53.7)	0.301
Family history of CMP or SCD	8 (5.3)	5 (4.1)	0.633
History of atrial fibrillation	45 (29.8)	29 (23.6)	0.248
Baseline LVEF, %	28.7 ± 8.7	24.1 ± 7.2	< 0.001†
Baseline LVEDDi, mm/m^2	37.0 ± 7.0	38.9 ± 6.0	< 0.001†
Follow-up interval, mo*	11 (8–13.5)	11 (8–13)	0.963
CMR data			
LVEF, %	28.6 ± 9.2	24.2 ± 8.2	< 0.001†
LVEDVi, mL/m^2	146.8 ± 49.6	166.4 ± 47.6	0.001†
LGE presence	74 (49)	51 (41.5)	0.212
LGE extent, %	7.6 ± 12.7	3.3 ± 7.0	0.014†
LGE location			0.100
Absent	77 (51)	72 (58.5)	
Septal wall only	35 (23.2)	27 (22)	
Non-septal wall only	9 (6)	6 (4.9)	
Both walls	21 (13.9)	6 (4.9)	
RVIP only	9 (6)	12 (9.8)	
LGE pattern			0.003†
Absent	77 (51)	72 (58.5)	
Mid-wall	40 (26.5)	22 (17.9)	
Multiple	19 (12.6)	5 (4.1)	
Subepicardial	1 (0.7)	0	
Focal	14 (9.3)	24 (19.5)	
Septal mid-wall LGE			0.014†
No	96 (63.6)	96 (78)	
Yes	55 (36.4)	27 (22)	
Native T1 (septal), ms	1344.8 ± 84.6	1352.2 ± 73.9	0.441

Data are mean ± standard deviation or n (%), unless specified otherwise. *Median (Q1–Q3), †Statistically significant. LVRR = left ventricular reverse remodeling, CMP = cardiomyopathy, CMR = cardiac magnetic resonance, eGFR = estimated glomerular filtration rate, LGE = late gadolinium enhancement, LVEDDi = left ventricular end-diastolic diameter index, LVEDVi = lveft ventricular end-diastolic volume index, LVEF = left ventricular ejection fraction, NT-proBNP = N-terminal (NT)-prohormone B-type natriuretic peptide, SCD = sudden cardiac death, RVIP = right ventricular insertion point

https://doi.org/10.3348/kjr.2023.0065

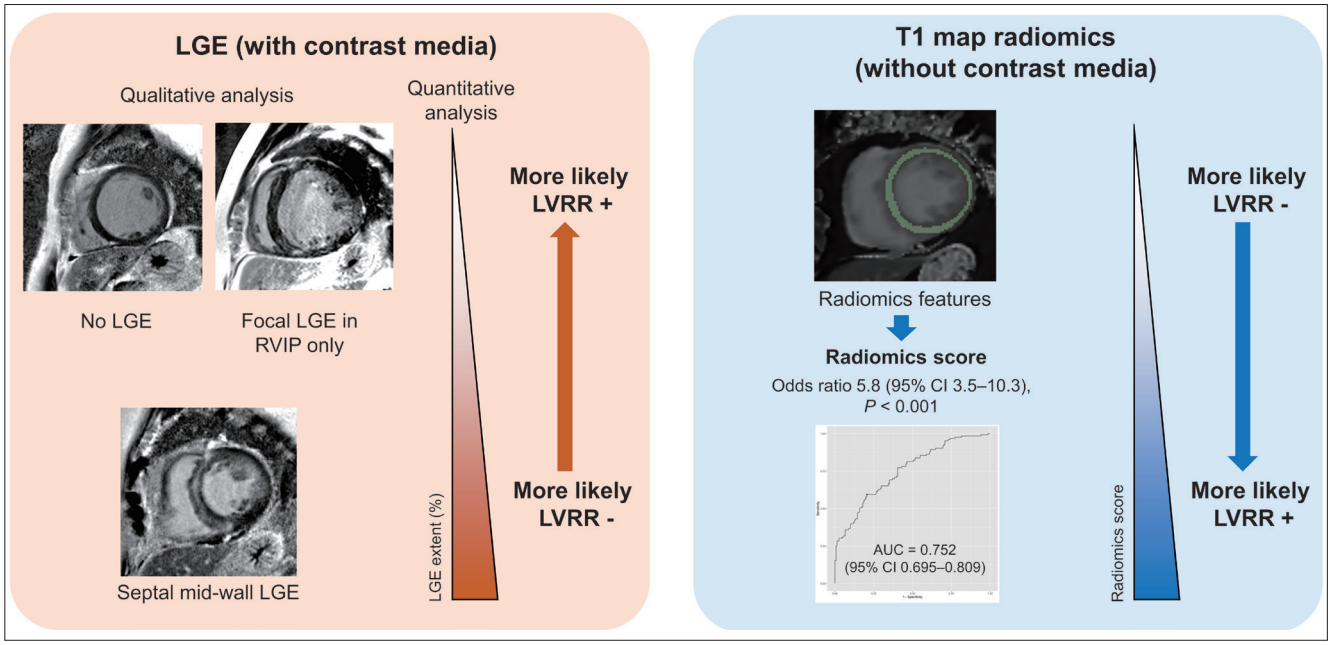

Fig. 3. Cardiac magnetic resonance-based tissue characterization and prediction of left ventricular reverse remodeling (LVRR) using late gadolinium enhancement (LGE) images and native T1 map. The extent of LGE had a negative association, whereas the radiomics score was positively associated with LVRR. Septal mid-wall LGE was more frequent in the LVRR-positive group, while no or focal LGE only in right ventricular insertion point (RVIP) was more frequent in the LVRR-negative group. AUC = area under the receiver operating characteristic curve, CI = confidence interval

Selection of Radiomics Features

A total of 869 radiomic features were extracted from native T1 map ROIs (Supplementary Table 1). After the feature selection process, 16 radiomic features were selected to construct a model to predict LVRR (Supplementary Table 2). These consisted of 12 texture features and four first-order features with various filters. The rad-score was significantly higher in the LVRR positive group than in the LVRR-negative group (0.1547 ± 0.8139 vs. -0.4980 ± 0.5344, $P < 0.001$; Fig. 4).

Prediction Models for LVRR

Table 2 shows the results of the univariable logistic regression analysis of clinical and radiologic variables for the prediction of LVRR. For clinical data, Ln NT-proBNP showed significant association with LVRR (odds ratio [OR], 1.3; 95% CI, 1.1–1.5; $P = 0.007$). Among the echocardiographic data, baseline LVEF (OR, 0.9; 95% CI, 0.9–1.0; $P < 0.001$) and LVEDDi (OR, 1.05; 95% CI, 1.01–1.09; $P = 0.016$) were significantly associated with LVRR. Among the conventional CMR data, LGE extent (OR, 0.95; 95% CI, 0.92–0.98; $P = 0.002$), both-wall LGE (OR, 0.3; 95% CI, 0.1–0.8, $P = 0.016$), multiple-pattern LGE (OR, 0.3; 95% CI, 0.1–0.7; $P = 0.016$), and septal mid-wall LGE (OR, 0.5; 95% CI, 0.3–0.8; $P = 0.01$) were significantly associated with LVRR. The optimal cut-off value of the LGE extent for predicting LVRR was 5.9% (sensitivity, 0.821; specificity, 0.377). The rad-score (OR, 5.8; 95% CI, 3.5–10.3; $P < 0.001$) also showed significant association with LVRR. The optimal cut-off value for LVRR was -0.041 (sensitivity, 0.593; specificity, 0.795).

Table 3 shows performance of the prediction model for LVRR. Table 4 shows the comparison of the performance of the prediction models for LVRR. The optimism-corrected AUC of the clinical + radiomic model was significantly higher than that of the clinical + LGE model (0.794 vs. 0.716; difference, 0.078; 99% CI, 0.003–0.151). The clinical + LGE + radiomics model showed significantly higher optimism-corrected AUC than the clinical + LGE model (0.811 vs. 0.716; difference, 0.095 [99% CI, 0.022–0.139]).

DISCUSSION

In this study, we developed and internally validated prediction models for LVRR using clinical and CMR data with T1 map radiomics. We identified 16 radiomics features extracted from the native T1 map that showed an independent prognostic association. We found that a combination of clinical data and radiomics features

https://doi.org/10.3348/kjr.2023.0065

Korean Journal of Radiology
KJR

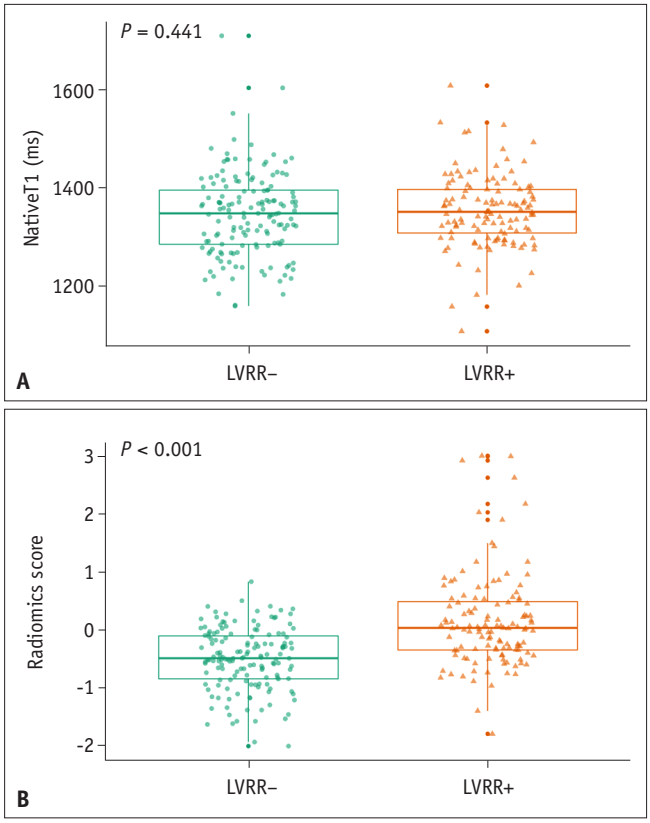

Fig. 4. Box plots for comparison of native T1 value and radiomics score in left ventricular reverse remodeling (LVRR) negative and positive groups. **A:** The native T1 value was not significantly different between the LVRR positive and LVRR negative group (1352.2 ± 73.9 ms vs. 1344.8 ± 84.6 ms, $P = 0.441$). **B:** The radiomics score was significantly higher in the LVRR positive group than in the LVRR-negative group (0.155 ± 0.814 vs. -0.498 ± 0.534, $P < 0.001$). *P* values were derived from independent *t*-tests.

predicted LVRR better than the model using clinical and LGE data without contrast media. Moreover, radiomics had an incremental prognostic value over clinical or conventional CMR information.

Since LVRR is an independent predictor of long-term prognosis [2], early identification of LVRR could help in clinical decision-making in patients with NIDCM. In our study, LVRR was present in 44.9% (123/274) of the patients at follow-up, which is similar to previous studies that showed LVRR in 31%–48% of patients with NIDCM [5-7,23]. Regarding clinical variables, prior studies revealed that systolic blood pressure [2,4], BNP [4,5], and baseline LVEF [6,7] were significantly associated with LVRR. Similarly, NT-proBNP level, baseline LVEF, and baseline LVEDDi were significantly associated with LVRR in univariable logistic regression analysis in our study.

The absence of baseline LGE has been reported as a

Table 2. Univariable Logistic Regression Analysis of Clinical and CMR Variables for Prediction of Left Ventricular Reverse Remodeling

Variables	Odds Ratio	95% CI	*P*
Clinical data			
Sex (male vs. female)*	1.2	0.7–1.9	0.502
Age, yr†	0.99	0.98–1.00	0.166
BMI, kg/m²†	1.01	0.96–1.06	0.740
Systolic blood pressure, mmHg†	1.01	1.00–1.02	0.076
Diastolic blood pressure, mmHg†	1.01	0.99–1.03	0.197
Creatinine, mg/dL†	1.2	1.0–1.7	0.127
eGFR, mL/min/1.73 m²†	1.0	0.99–1.01	0.627
Sodium, mmol/L†	1.0	0.99–1.02	0.606
Ln NT-proBNP, pg/mL†	1.3	1.1–1.5	0.007‡
Diabetes (yes vs. no)*	0.7	0.4–1.3	0.324
Smoking (yes vs. no)*	1.5	0.9–2.4	0.122
Family history of CMP or SCD (yes vs. no)*	0.8	0.2–2.3	0.634
History of atrial fibrillation (yes vs. no)*	0.7	0.4–1.2	0.249
Baseline LVEF, %†	0.9	0.9–1.0	< 0.001‡
Baseline LVEDDi, mm/m²†	1.05	1.01–1.09	0.016‡
CMR data			
LGE presence (yes vs. no)*	0.7	0.5–1.2	0.213
LGE extent, %†	0.95	0.92–0.98	0.002‡
LGE location			
Absent	Reference		
Septal wall only	0.8	0.5–1.5	0.527
Non-septal wall only	0.7	0.2–2.1	0.540
Both walls	0.3	0.1–0.8	0.016‡
RVIP only	1.4	0.6–3.7	0.451
LGE pattern			
Absent	Reference		
Mid-wall	0.6	0.3–1.1	0.089
Multiple	0.3	0.1–0.7	0.016‡
Subepicardial	0	NA–6.8e+71	0.987
Focal	1.8	0.9–3.9	0.105
Septal mid-wall LGE (yes vs. no)*	0.5	0.3–0.8	0.010†
Native T1 (septal), ms†	1.0	1.0–1.0	0.439
Radiomics score†	5.8	3.5–10.3	< 0.001‡

*For categorical variables with categories in parentheses, the former was compared with the latter (reference) to calculate odds ratios and 95% CIs with the logistic regression analysis, †For continuous variables, an increase by 1 considered when calculating odds ratios and 95% CIs with the logistic regression analysis, ‡Statistically significant. BMI = body mass index, CMP = cardiomyopathy, CMR = cardiac magnetic resonance, eGFR = estimated glomerular filtration rate, LGE = late gadolinium enhancement, LVEDDi = left ventricular end-diastolic diameter index, LVEF = left ventricular ejection fraction, NT-proBNP = N-terminal (NT)-prohormone B-type natriuretic peptide, SCD = sudden cardiac death, CI = confidence interval, RVIP = right ventricular insertion point, NA = not applicable

https://doi.org/10.3348/kjr.2023.0065

predictive factor for LVRR in previous studies of DCM patients [6,7]. However, one study reported that the presence of LGE was not associated with adverse events in DCM patients [24]. In our results, LGE was more frequent in the LVRR-negative group; however, it was not significantly associated with LVRR and could not be included in the prediction model. The

Table 3. Model Performances Measured by AUC for Prediction of Left Ventricular Reverse Remodeling

Model	Included Features	Variables	Beta	*P*	Apparent AUC (95% CI)	Optimism-corrected AUC (95% CI)
One layer						
Model 1a	Clinical	Intercept	-4.145	0.013	0.695 (0.631–0.760)	0.676 (0.616–0.741)
		Systolic blood pressure	0.032	0.001*		
		LVEF	-0.075	< 0.001*		
		LVEDDi	0.054	0.023*		
		Smoking (yes)	0.408	0.152		
Model 1b	Radiomics	Intercept	0.164	0.270	0.752 (0.695–0.809)	0.753 (0.698–0.813)
		Radiomics score	1.758	< 0.001*		
Two layers						
Model 2a	Clinical + LGE	Intercept	4.621	0.008	0.739 (0.679–0.800)	0.716 (0.657–0.779)
		Systolic blood pressure	0.030	0.002*		
		LVEF	-0.073	< 0.001*		
		LVEDDi	0.078	0.003*		
		Smoking (yes)	0.531	0.074		
		LGE extent (%)	-0.052	0.011*		
		Septal mid-wall LGE	-0.233	0.540		
Model 2b	Clinical + Radiomics	Intercept	-0.588	0.758	0.808 (0.756–0.86)	0.794 (0.744–0.845)
		Systolic blood pressure	0.012	0.275		
		LVEF	-0.089	< 0.001*		
		LVEDDi	0.041	0.105		
		Smoking (yes)	0.324	0.314		
		Radiomics score	1.937	< 0.001*		
Three layers						
Model 3	Clinical + LGE + Radiomics	Intercept	-0.969	0.622	0.829 (0.779–0.878)	0.811 (0.763–0.862)
		Systolic blood pressure	0.010	0.366		
		LVEF	-0.085	< 0.001*		
		LVEDDi	0.059	0.032*		
		Smoking (yes)	0.421	0.204		
		LGE extent (%)	-0.044	0.041*		
		Septal mid-wall LGE	-0.139	0.743		
		Radiomics score	1.825	< 0.001*		

*Statistically significant. AUC = area under the receiver operating characteristic curve, CI = confidence interval, LGE = late gadolinium enhancement, LVEDDi = left ventricular end-diastolic diameter index, LVEF = left ventricular ejection fraction

Table 4. Comparison of Model Performances Measured by AUCs in the Prediction of Left Ventricular Reverse Remodeling

First Model	Second Model	Adjusted *P** for Comparison of AUC	Difference between Optimism-corrected AUC (99% CI†)
Clinical	Clinical + LGE	0.100	0.040 (-0.026–0.074)
Clinical	Clinical + Radiomics	< 0.001‡	0.118 (0.036–0.172)‡
Clinical + LGE	Clinical + Radiomics	0.061	0.078 (0.003–0.151)‡
Clinical + LGE	Clinical + LGE + Radiomics	< 0.001‡	0.095 (0.022–0.139)‡
Clinical + Radiomics	Clinical + LGE + Radiomics	0.271	0.016 (-0.021–0.033)

*Adjusted *P* value using Bonferroni correction for multiple comparisons (raw *P* value*5), †The optimism-corrected AUC difference was calculated as second model – first model with 1000 times bootstrapping. Bonferroni correction was applied for multiple comparisons (alpha = 0.05/10 = 0.005), ‡Statistically significant. AUC = area under the receiver operating characteristic curve, CI = confidence interval, LGE = late gadolinium enhancement

https://doi.org/10.3348/kjr.2023.0065

Korean Journal of Radiology
KJR

presence of LGE is subjectively determined by the reader and has potential inter-observer variability, especially in cases with mild LGE. In this regard, quantification of the extent of LGE might be a more objective tool than the 'presence' of LGE. In our study, LGE extent was significantly associated with LVRR in univariable logistic regression, which is consistent with the results of previous studies [5,23,24]. In terms of the location or pattern of LGE, both wall location and multiple patterns of LGE were negatively associated with LVRR. The presence of septal mid-wall LGE was negatively associated with LVRR, which is consistent with a previous study that reported septal wall LGE as an important prognostic factor in DCM patients [25]. However, LGE focally located or located only in the RVIP was not negatively associated with LVRR and was more frequently observed in the LVRR-positive group than in the LVRR-negative group. This result is in line with previous studies that reported that LGE confined to the RVIP had no significant association with adverse cardiac events in patients with NIDCM [26,27]. LGE in RVIP appeared to have a different histological substrate compared to LGE in other locations [27], resulting in different clinical significance in NIDCM patients.

Although the LGE pattern and location are beneficial for prognosis prediction, they can be subjective because they are qualitative assessments. The LGE extent has an advantage in that it can be quantified, but this extent varies significantly with the quantification method used and has limited reproducibility [28]. Moreover, the use of contrast media is limited in patients with reduced renal function. In addition, enhanced images may vary depending on renal function, delay time after contrast administration, and characteristics of contrast agents, such as dose or concentration. Therefore, it is desirable to identify and characterize myocardial fibrosis using images without contrast enhancement. Myocardial mapping can be more useful for the standardization and evaluation of the physical properties of tissues. However, in our study, the mean native T1 value was not significantly associated with LVRR, as shown in a previous study [7], and was not included in the prediction model. Though the reason remains unclear, a possible explanation for this may be that the mean value alone cannot reflect the tissue heterogeneity caused by myocardial fibrosis.

Our study demonstrated the incremental prognostic value of radiomics features from a native T1 map over clinical or conventional CMR data for the prediction of LVRR. This is particularly meaningful in that T1 map radiomics allows prognostic prediction without using contrast media. Our results are in line with recently published studies that suggested the importance of tissue heterogeneity on the native T1 map for predicting prognosis in patients with NIDCM [14,15]. The relevant radiomics features selected in our study to predict LVRR were 12 texture features and four first-order features. A previous prognostic radiomics study using LGE images also reported three important features selected from texture features [24]. Texture features reflect myocardial heterogeneity [29]. Myocardial interstitial fibrosis is a heterogeneous process that can occur as a combination of interstitial microscars, perivascular collagen fiber deposition, and increased thickness of mysial collagen strands [30]. Fibrosis heterogeneity in the myocardium is related to the risk of adverse events [31]. A previous study also showed that LV entropy, a source of myocardial heterogeneity, was associated with arrhythmic events in patients with DCM receiving defibrillators for the primary prevention of sudden cardiac death [32]. First-order features represent voxel intensity, generally obtained from histogram-based methods [33]. In the native T1 map, the signal intensity was related to diffuse myocardial fibrosis [34]. Consequently, radiomics features composed of quantitative imaging data reflect myocardial heterogeneity and interstitial fibrosis, which are associated with the prognosis of NIDCM. Altogether, our results imply that radiomics has potential as a novel imaging biomarker for improving risk stratification and personalizing the treatment of patients with NIDCM.

This study has several limitations. First, this was a single-center study with a retrospective design, and we did not perform external validation with independent datasets for generalization. Further validation in an external dataset is needed with the standardization of the CMR protocol. Second, ROI placement was manually drawn using a reader, which can produce inter-observer variability. Automated segmentation based on a deep-learning method can provide further workflow automation and minimize user bias. Third, we did not include strain echocardiography, T2, or extracellular volume fraction, which may have influenced the results.

In conclusion, according to this single-center study, the radiomics characteristics extracted from a non-enhanced T1 map may improve the prediction of LVRR and offer added value over traditional LGE in patients with NIDCM. Additional external validation research is required.

 https://doi.org/10.3348/kjr.2023.0065

Supplement

The Supplement is available with this article at https://doi.org/10.3348/kjr.2023.0065.

Availability of Data and Material

The datasets are available from the corresponding author on reasonable request.

Conflicts of Interest

Kyunghwa Han, a contributing editor of the *Korean Journal of Radiology*, was not involved in the editorial evaluation or decision to publish this article. All remaining authors have declared no conflicts of interest.

Author Contributions

Conceptualization: Suyon Chang, Byoung Wook Choi. Data curation: Suyon Chang. Formal analysis: Suyon Chang, Lina Kim, Seunghyun Hwang, Kyunghwa Han, Hwiyoung Kim, Yonghan Kwon. Funding acquisition: Byoung Wook Choi. Investigation: Suyon Chang, Byoung Wook Choi. Methodology: Suyon Chang, Byoung Wook Choi. Project administration: Byoung Wook Choi. Supervision: Byoung Wook Choi. Validation: Suyon Chang, Kyunghwa Han, Yonghan Kwon. Visualization: Suyon Chang. Writing—original draft: Suyon Chang. Writing—review & editing: all authors.

ORCID iDs

Suyon Chang
https://orcid.org/0000-0002-9221-8116
Kyunghwa Han
https://orcid.org/0000-0002-5687-7237
Yonghan Kwon
https://orcid.org/0000-0001-7951-1142
Lina Kim
https://orcid.org/0009-0000-9582-1693
Seunghyun Hwang
https://orcid.org/0000-0002-5900-6445
Hwiyoung Kim
https://orcid.org/0000-0001-7778-8973
Byoung Wook Choi
https://orcid.org/0000-0002-8873-5444

Funding Statement

This research was supported by the National Research Foundation of Korea (NRF) grant funded by the Ministry of Science and ICT (NRF-2018M3A9H6081483 & NRF-2017R1D1A1B03035136).

REFERENCES

1. Elliott P, Andersson B, Arbustini E, Bilinska Z, Cecchi F, Charron P, et al. Classification of the cardiomyopathies: a position statement from the European Society of Cardiology Working Group on myocardial and pericardial diseases. *Eur Heart J* 2008;29:270-276
2. Merlo M, Pyxaras SA, Pinamonti B, Barbati G, Di Lenarda A, Sinagra G. Prevalence and prognostic significance of left ventricular reverse remodeling in dilated cardiomyopathy receiving tailored medical treatment. *J Am Coll Cardiol* 2011;57:1468-1476
3. Hoshikawa E, Matsumura Y, Kubo T, Okawa M, Yamasaki N, Kitaoka H, et al. Effect of left ventricular reverse remodeling on long-term prognosis after therapy with angiotensin-converting enzyme inhibitors or angiotensin II receptor blockers and β blockers in patients with idiopathic dilated cardiomyopathy. *Am J Cardiol* 2011;107:1065-1070
4. Choi JO, Kim EY, Lee GY, Lee SC, Park SW, Kim DK, et al. Predictors of left ventricular reverse remodeling and subsequent outcome in nonischemic dilated cardiomyopathy. *Circ J* 2013;77:462-469
5. Kubanek M, Sramko M, Maluskova J, Kautznerova D, Weichet J, Lupinek P, et al. Novel predictors of left ventricular reverse remodeling in individuals with recent-onset dilated cardiomyopathy. *J Am Coll Cardiol* 2013;61:54-63
6. Masci PG, Schuurman R, Andrea B, Ripoli A, Coceani M, Chiappino S, et al. Myocardial fibrosis as a key determinant of left ventricular remodeling in idiopathic dilated cardiomyopathy: a contrast-enhanced cardiovascular magnetic study. *Circ Cardiovasc Imaging* 2013;6:790-799
7. Xu Y, Li W, Wan K, Liang Y, Jiang X, Wang J, et al. Myocardial tissue reverse remodeling after guideline-directed medical therapy in idiopathic dilated cardiomyopathy. *Circ Heart Fail* 2021;14:e007944
8. Alba AC, Gaztañaga J, Foroutan F, Thavendiranathan P, Merlo M, Alonso-Rodriguez D, et al. Prognostic value of late gadolinium enhancement for the prediction of cardiovascular outcomes in dilated cardiomyopathy: an international, multi-institutional study of the MINICOR group. *Circ Cardiovasc Imaging* 2020;13:e010105
9. Kim C, Park CH, Kim DY, Cha J, Lee BY, Park CH, et al. Semi-quantitative scoring of late gadolinium enhancement of the left ventricle in patients with ischemic cardiomyopathy: improving interobserver reliability and agreement using consensus guidance from the Asian Society of Cardiovascular Imaging-Practical Tutorial (ASCI-PT) 2020. *Korean J Radiol* 2022;23:298-307
10. Li S, Zhou D, Sirajuddin A, He J, Xu J, Zhuang B, et al. T1 mapping and extracellular volume fraction in dilated cardiomyopathy: a prognosis study. *JACC Cardiovasc Imaging* 2022;15:578-590

11. Nakamori S, Bui AH, Jang J, El-Rewaidy HA, Kato S, Ngo LH, et al. Increased myocardial native T1 relaxation time in patients with nonischemic dilated cardiomyopathy with complex ventricular arrhythmia. *J Magn Reson Imaging* 2018;47:779-786
12. Parmar C, Leijenaar RT, Grossmann P, Rios Velazquez E, Bussink J, Rietveld D, et al. Radiomic feature clusters and prognostic signatures specific for lung and head & neck cancer. *Sci Rep* 2015;5:11044
13. Lambin P, Rios-Velazquez E, Leijenaar R, Carvalho S, van Stiphout RG, Granton P, et al. Radiomics: extracting more information from medical images using advanced feature analysis. *Eur J Cancer* 2012;48:441-446
14. Kinoshita M, Kato S, Kodama S, Azuma M, Nakayama N, Fukui K, et al. Native T1 heterogeneity for predicting reverse remodeling in patients with non-ischemic dilated cardiomyopathy. *Heart Vessels* 2022;37:1541-1550
15. Nakamori S, Ngo LH, Rodriguez J, Neisius U, Manning WJ, Nezafat R. T1 mapping tissue heterogeneity provides improved risk stratification for ICDs without needing gadolinium in patients with dilated cardiomyopathy. *JACC Cardiovasc Imaging* 2020;13:1917-1930
16. Schulz-Menger J, Bluemke DA, Bremerich J, Flamm SD, Fogel MA, Friedrich MG, et al. Standardized image interpretation and post-processing in cardiovascular magnetic resonance - 2020 update. *J Cardiovasc Magn Reson* 2020;22:19
17. Beare R, Lowekamp B, Yaniv Z. Image segmentation, registration and characterization in R with SimpleITK. *J Stat Softw* 2018;86:8
18. Zwanenburg A, Vallières M, Abdalah MA, Aerts HJWL, Andrearczyk V, Apte A, et al. The image biomarker standardization initiative: standardized quantitative radiomics for high-throughput image-based phenotyping. *Radiology* 2020;295:328-338
19. Shafiq-Ul-Hassan M, Zhang GG, Latifi K, Ullah G, Hunt DC, Balagurunathan Y, et al. Intrinsic dependencies of CT radiomic features on voxel size and number of gray levels. *Med Phys* 2017;44:1050-1062
20. Collewet G, Strzelecki M, Mariette F. Influence of MRI acquisition protocols and image intensity normalization methods on texture classification. *Magn Reson Imaging* 2004;22:81-91
21. Han K, Song K, Choi BW. How to develop, validate, and compare clinical prediction models involving radiological parameters: study design and statistical methods. *Korean J Radiol* 2016;17:339-350
22. Collins GS, Reitsma JB, Altman DG, Moons KG. Transparent reporting of a multivariable prediction model for individual prognosis or diagnosis (TRIPOD). *Ann Intern Med* 2015;162:735-736
23. Ishii S, Inomata T, Fujita T, Iida Y, Ikeda Y, Nabeta T, et al. Clinical significance of endomyocardial biopsy in conjunction with cardiac magnetic resonance imaging to predict left ventricular reverse remodeling in idiopathic dilated cardiomyopathy. *Heart Vessels* 2016;31:1960-1968
24. Shu S, Wang C, Hong Z, Zhou X, Zhang T, Peng Q, et al. Prognostic value of late enhanced cardiac magnetic resonance imaging derived texture features in dilated cardiomyopathy patients with severely reduced ejection fractions. *Front Cardiovasc Med* 2021;8:766423
25. Halliday BP, Baksi AJ, Gulati A, Ali A, Newsome S, Izgi C, et al. Outcome in dilated cardiomyopathy related to the extent, location, and pattern of late gadolinium enhancement. *JACC Cardiovasc Imaging* 2019;12(8 Pt 2):1645-1655
26. Yi JE, Park J, Lee HJ, Shin DG, Kim Y, Kim M, et al. Prognostic implications of late gadolinium enhancement at the right ventricular insertion point in patients with non-ischemic dilated cardiomyopathy: a multicenter retrospective cohort study. *PLoS One* 2018;13:e0208100
27. Claver E, Di Marco A, Brown PF, Bradley J, Nucifora G, Ruiz-Majoral A, et al. Prognostic impact of late gadolinium enhancement at the right ventricular insertion points in non-ischaemic dilated cardiomyopathy. *Eur Heart J Cardiovasc Imaging* 2023;24:346-353
28. Flett AS, Hasleton J, Cook C, Hausenloy D, Quarta G, Ariti C, et al. Evaluation of techniques for the quantification of myocardial scar of differing etiology using cardiac magnetic resonance. *JACC Cardiovasc Imaging* 2011;4:150-156
29. Hassani C, Saremi F, Varghese BA, Duddalwar V. Myocardial radiomics in cardiac MRI. *AJR Am J Roentgenol* 2020;214:536-545
30. Díez J, González A, Kovacic JC. Myocardial interstitial fibrosis in nonischemic heart disease, part 3/4: JACC focus seminar. *J Am Coll Cardiol* 2020;75:2204-2218
31. Wu KC. Sudden cardiac death substrate imaged by magnetic resonance imaging: from investigational tool to clinical applications. *Circ Cardiovasc Imaging* 2017;10:e005461
32. Muthalaly RG, Kwong RY, John RM, van der Geest RJ, Tao Q, Schaeffer B, et al. Left ventricular entropy is a novel predictor of arrhythmic events in patients with dilated cardiomyopathy receiving defibrillators for primary prevention. *JACC Cardiovasc Imaging* 2019;12(7 Pt 1):1177-1184
33. Gillies RJ, Kinahan PE, Hricak H. Radiomics: images are more than pictures, they are data. *Radiology* 2016;278:563-577
34. Nakamori S, Dohi K, Ishida M, Goto Y, Imanaka-Yoshida K, Omori T, et al. Native T1 mapping and extracellular volume mapping for the assessment of diffuse myocardial fibrosis in dilated cardiomyopathy. *JACC Cardiovasc Imaging* 2018;11:48-59

https://doi.org/10.3348/kjr.2023.0065